Progress in Organic Coatings 222 (2027) 110687

Contents lists available at ScienceDirect

Progress in Organic Coatings

journal homepage: www.elsevier.com/locate/porgcoat

# Bio-based UV-curable vitrimeric coatings incorporating DNA for enhanced flame retardancy and circularity

Luigi Gamberini [a], Anna Liguori [a,*], Daniele Battegazzore [b], Giulio Malucelli [b,*], Maria Letizia Focarete [a,c]

[a] Department of Chemistry "Giacomo Ciamician" and INSTM UdR of Bologna, University of Bologna, via P. Gobetti 85, Bologna, 40129, Italy
[b] Department of Applied Science and Technology, Politecnico di Torino, Viale Teresa Michel 5, Alessandria, 15121, Italy
[c] Health Sciences & Technologies (HST) CIRI, University of Bologna, Via Tolara di Sopra 41/E, Ozzano Emilia, 40064, Italy

ARTICLE INFO

*Keywords:*
UV-curable vitrimeric coatings
DNA
Bio-based flame retardants
Cone calorimetry
Pyrolysis-combustion flow calorimetry
Healable coatings
Recyclable coatings

ABSTRACT

The development of multifunctional UV-cured coating formulations combining sustainability, flame retardancy, and circularity remains a major challenge for advanced polymeric materials. In this work, a fully bio-based UV-curable vitrimeric formulation was developed by combining a vanillin-derived Schiff-base resin with DNA from herring sperm as a sustainable intumescent flame-retardant additive. DNA was incorporated at 10 and 20% w/w, and the resulting UV-cured coating formulations were investigated in terms of morphology, thermomechanical properties, flame-retardant performance, thermally activated scratch closure, and chemical recyclability. SEM observations revealed a heterogeneous morphology arising from the limited compatibility between DNA and the hydrophobic vitrimeric matrix, while DSC and DMTA demonstrated that DNA slightly increased the glass transition temperature and storage modulus without preventing network formation. TGA showed a marked increase in char residue. Cone calorimetry revealed progressive reductions of 38% in peak heat release rate, 46% in total heat release, and 73% in total smoke release for the formulation containing 20% w/w DNA relative to the unfilled formulation. PCFC results showed a similar trend. However, all formulations remained not classified in UL-94 vertical flame-spread tests. SEM-EDS analyses of combustion residues revealed a more compact, phosphorus-rich char, consistent with a predominantly char-forming contribution of DNA in the condensed phase. DNA incorporation did not prevent repeated thermally activated scratch closure or chemical recycling through transimination. Although scratch closure at 120 °C may be the synergic effect of dynamic bond exchange and thermally activated polymer mobility, these findings demonstrate the potential of DNA-containing imine vitrimers as sustainable UV-cured coating formulations with improved fire performance and circularity.

## 1. Introduction

Polymeric coatings are extensively employed in numerous industrial sectors, including construction, transportation, electronics, and consumer products, owing to their ability to protect substrates against corrosion, abrasion, moisture sorption, and environmental degradation [1,2]. In many of these applications, coatings are also required to provide effective fire protection, reducing flame spread and heat release during combustion [3,4]. Therefore, the development of flame retardant coatings has become an increasingly important research topic, driven by both safety requirements and the growing demand for environmentally sustainable materials. Conventional flame retardant (FR) systems are commonly based on synthetic phosphorus-containing additives [5,6]. Although highly effective, these materials often raise environmental concerns due to their persistence, and the potential generation of hazardous degradation products during combustion [7]. As a consequence, significant efforts are being devoted to the identification of renewable and environmentally benign alternatives capable of providing comparable fire performance while reducing the ecological footprint of FR formulations. Among the various bio-based flame retardants investigated in recent years, deoxyribonucleic acid (DNA) has emerged as a particularly promising candidate [8]. DNA possesses a unique chemical structure that resembles an intumescent FR system at the molecular level. Its phosphate backbone acts as a dehydrating acid source, the deoxyribose units behave as a carbon source, and the nitrogen-containing nucleobases function as blowing agents. Upon heating,

* Corresponding authors.
*E-mail addresses:* anna.liguori@unibo.it (A. Liguori), giulio.malucelli@polito.it (G. Malucelli).

https://doi.org/10.1016/j.porgcoat.2026.110687
Received 22 July 2026; Received in revised form 2 October 2026; Accepted 12 October 2026
Available online 23 October 2026
0300-9440/© 2026 The Author(s). Published by Elsevier B.V. This is an open access article under the CC BY license (http://creativecommons.org/licenses/by/4.0/).

these components cooperate to promote dehydration and charring reactions while releasing non-flammable gases, leading to the formation of an expanded protective carbonaceous (char) layer [9]. Owing to this intrinsic intumescent behavior, DNA has successfully been employed to improve the fire performance of textiles, thermoplastic polymers, and thermosetting resins. In addition, DNA can be obtained from industrial waste streams, such as fish-processing by-products, further enhancing its attractiveness from a sustainability perspective. Alongi et al. demonstrated that DNA can significantly improve the fire resistance of cotton fabrics, leading to self-extinction and remarkable reductions in flammability [10]. The intrinsic intumescent nature of DNA promoted the formation of a protective char layer that reduced heat and mass transfer, thereby suppressing combustion and limiting flame propagation. The applicability of DNA as a FR additive has been extended to several thermoplastic polymers, including ethylene-vinyl acetate, polypropylene and acrylonitrile-butadiene-styrene copolymers, polyethylene terephthalate, and polyamide 6, demonstrating that DNA coatings were able to significantly improve the fire performance of all investigated substrates by delaying ignition and reducing the peak heat release rate during cone calorimetry tests [11]. The application of DNA as a FR additive has also been extended to thermosetting polymers. Zabihi et al. [12] developed epoxy nanocomposites containing DNA-modified clay nanoparticles and demonstrated that the incorporation of DNA significantly enhanced both the thermal stability and fire performance of the epoxy matrix. Compared with conventional organoclay-filled systems, the DNA-modified nanocomposites exhibited higher char yields, delayed thermal degradation, and reduced heat release during combustion. In particular, cone calorimetry tests revealed a 21% reduction in peak heat release rate (PHRR) and a 31% decrease in total heat release (THR) for systems containing 2.5% w/w DNA-modified clay compared to pure epoxy. These improvements were accompanied by a substantial increase in char yield, from 0.75% to 13.3%, and by the formation of compact and coherent char layers acting as effective barriers against heat and mass transfer during combustion.

In parallel with the development of sustainable flame-retardant systems, increasing attention is being devoted to polymeric materials designed according to circular-economy principles. In this context, vitrimers have emerged as a particularly attractive class of covalent adaptable networks [13–15]. Unlike conventional thermosets, vitrimers can undergo topology rearrangements through dynamic covalent bond-exchange reactions while maintaining their crosslinked structure. This peculiar behavior can enable stress relaxation, healing, reshaping, reprocessing, and chemical recycling, thereby extending the material's lifetime and reducing waste generation [16–18]. The integration of flame retardancy and vitrimer chemistry is receiving increasing attention, including in recent phosphorus-nitrogen-containing systems [19,20]. However, the use of biomass-derived DNA as an intumescent additive in a bio-based UV-curable imine vitrimer remains largely unexplored.

Therefore, in this work, a vanillin-derived Schiff-base resin was selected as a fully bio-based, UV-curable matrix containing dynamic imine bonds, enabling the combined investigation of flame retardancy, thermally activated scratch closure, and chemical recycling. To this aim, DNA from herring sperm was incorporated as a physically dispersed, bio-based flame retardant additive. Although the polarity mismatch between hydrophilic DNA and the hydrophobic resin was expected to limit molecular-level compatibility, this combination was deliberately explored to assess whether DNA could retain its char-forming function in a vitrimeric coating matrix. The resulting UV-cured coating formulations and free-standing films were investigated in terms of morphology, thermomechanical behavior, solvent resistance, fire performance, scratch closure, and chemical recycling. The results show that DNA improves forced-combustion performance while preserving the characteristic circularity of the vitrimeric matrix, providing a proof of concept for sustainable UV-cured coating formulations.

## 2. Experimental section

### 2.1. Materials

Vanillin (VL, >99%) and 2,2′-(Ethylenedioxy)bis(ethylamine) (DOM, 99%) were purchased from BLDpharm and used without any additional purification. Deoxyribonucleic acid from herring sperm (DNA) ("crude oligonucleotides", <50 bp), methacrylic anhydride (MAA, 94%), 4-dimethylaminopyridine (DMAP, 99%), sodium hydrogen carbonate (for analysis), sodium hydroxide (98%), sodium sulfate (≥99%), and dichloromethane (DCM, ≥99%) were purchased from Sigma-Aldrich and used as received. 2-Hydroxy-2-methyl-1-phenylpropanone (Irgacure 1173), used as photoinitiator, was kindly supplied by IGM Resins Italia (Mortara (PV), Italy). Microscope glass slides from Apta Slides were used as glass supports.

### 2.2. Synthesis of DOM-MVL

The CAN resin, DOM-MVL, was synthesized according to a double-step procedure consisting of the methacrylation of VL to produce methacrylated vanillin (MVL) and the subsequent Schiff-base reaction between MVL and DOM. MVL was obtained according to the previously reported procedure [21]. Briefly, VL (30.00 g, 197.17 mmol) was mixed with MAA (30.36 g, 197.00 mmol) and DMAP (0.17 g, 1.39 mmol) in a 250 mL round-bottom flask and kept under stirring at 60 °C for 24 h. The reaction product was diluted with DCM and subsequently washed with saturated aqueous sodium hydrogen carbonate, 0.5 M NaOH, 1 M NaOH, and distilled water. The organic phase was dried over $Na_2SO_4$, concentrated at reduced pressure, and dried under vacuum at room temperature for 2 days, yielding MVL as a white powder (81% reaction yield). The DOM-MVL resin was obtained by subjecting the MVL to a Schiff-base reaction with DOM [17,22–24]. In brief, MVL (4.05 g, 18.40 mmol) and DOM (1.78 g, 12.00 mmol) were placed in a 250 mL round-bottom flask and dissolved in 60 mL of DCM. The reaction was carried out at room temperature for 5 h under mechanical stirring. Afterward, the reaction mixture underwent to the same washing and drying procedures as described for methacrylation, yielding DOM-MVL as a pale-yellow oil (96% reaction yield).

### 2.3. Preparation of FR coatings and networks

DNA was dispersed in DOM-MVL resin by manual mixing. Three formulations were produced, namely: (i) unfilled DOM-MVL resin (without DNA), (ii) DOM-MVL resin incorporating 10% w/w DNA relative to the resin weight, (iii) DOM-MVL resin containing 20% w/w DNA relative to the resin weight. Hereafter, the coatings and free-standing films obtained from these formulations are referred to as DOM-MVL, DOM-MVL + 10% w/w DNA, and DOM-MVL + 20% w/w DNA, respectively. Irgacure 1173 was then added at a concentration of 4% w/w with respect to the weight of the resin and mixed manually together with the other components.

For the preparation of the coating on aluminum foils and on microscope glass substrates, the mixture was applied with a wire wound applicator (nominal thickness = 200 μm) and subsequently UV-cured using Heraeus Noblelight F300S UV Lamp System for 20 s (single exposure). Free-standing films were obtained by peeling the cured coatings off from the aluminum substrate, exploiting the higher stiffness of the cured material compared to the aluminum foil.

### 2.4. Chemical recycling

The possibility of chemically decomposing the coatings and removing them from glass substrates was also investigated. Glass substrates (2 cm × 3 cm) coated with DOM-MVL or DOM-MVL + 20% w/w DNA were immersed in 5 mL DOM and heated at 60 °C for 30 min. Subsequently, the glass substrate was removed and the resulting dark

orange solid precipitate was collected and dried under vacuum overnight. The recovered oligomeric fragments were subsequently employed for preparing recycled free-standing films. For the pristine system, 100 mg of the recovered oligomeric solid was mixed with 10 mg of MVL by grinding. The resulting powder was transferred in a Teflon mold and hot-pressed at 100 °C for 10 min under 20 bar. For the DOM-MVL + 20% DNA system, 100 mg of oligomeric solid was mixed with 10 mg of MVL and 28 mg of DNA by grinding. The mixture was then transferred in a Teflon mold and hot-pressed under the same conditions.

### 2.5. Characterization of resin, films, and coatings

The chemical structure of DOM-MVL was confirmed by means of $^1$H NMR spectroscopy performed on an Avance 600 (Bruker) spectrometer (600 MHz) equipped with a 5.0 mm multi-nuclear observe probe with *Z*-gradient. $CDCl_3$ was used as both solvent and internal reference for chemical shift calibration. The chemical structure of the coatings, oligomeric products deriving from coating decomposition, and the chemically recycled networks were investigated by means of ATR-FTIR using a Cary 630 FTIR Spectrometer (Agilent Technologies). All spectra were recorded in the wavenumber range of 4000–600 $cm^{-1}$ using 64 scans at a resolution of 4 $cm^{-1}$.

The morphological and microstructural features of the coatings were examined via a ZEISS EVO 15 SEM, equipped with an Oxford Ultim Max 40 EDX, employed for elemental composition analysis. Prior to the analyses, the coatings were coated with a thin gold layer.

The thermo-oxidative behavior of the free-standing films was investigated by means of a TGA Q550 apparatus (TA-Instruments). Samples with a weight within 8 and 12 mg were subjected to a heating scan from room temperature to 700 °C with a heating rate of 10 °C/min in air atmosphere. Differential scanning calorimetry (DSC) analysis of the films was performed using a DSC Q10 instrument (TA Instruments) equipped with a refrigerated cooling system (RCS) in $N_2$ atmosphere. About 15 mg of sample was sealed into an aluminum crucible and subjected to a heating scan from −90 °C to 150 °C with a heating rate of 20 °C/min. The glass transition temperature ($T_g$) was taken as the half-height of the glass transition heat capacity step. 20 mm × 5 mm specimens were analyzed by multi-frequency strain analyses, which were performed using a DMA Q800 apparatus (TA Instrument). The measurements were performed with a static force of 0.01 N, at a frequency of 1.0 Hz. The strain and Poisson's ratio were set at 0.1% and 0.44, respectively. The samples were equilibrated at −40 °C for 5 min and tested from −40 °C to 150 °C at 1 Hz with a 3 °C/min heating rate. The glass transition temperature was considered as the maximum of the tan δ curve.

Gel content measurements were carried out to investigate the solvent resistance of the free-standing networks by immersing each sample (around 30 mg) in 3 mL of solvent (i.e., DCM or and distilled $H_2O$) for 72 h at room temperature. After being removed from the solvent, the samples were dried in a vacuum oven at 60 °C until a constant weight was reached. The gel fraction was determined according to Eq. (1).

$$Gel\ content\% = \frac{m_f}{m_i} \times 100 \quad (1)$$

where $m_f$ is the final weight of the sample after 72 h of immersion, $m_i$ is the weight before the immersion. The analysis was performed in triplicate.

The fire behavior of the vitrimeric films was assessed through flammability and forced-combustion tests. The former were performed using vertical flame spread tests according to the UL94 standard; the latter involved both cone calorimetry (CC) and pyrolysis-combustion flow calorimetry (PCFC) tests. CC analyses were carried out using a cone calorimeter (Noselab Srl, Milano, Italy), according to ISO 5660; measurements were performed at 35 $kW/m^2$ irradiative heat flux on horizontally oriented specimens (50 × 50 mm). Three replicates were tested for each formulation. PCFC tests were performed according to the ASTM D7309 standard using a Micro Calorimeter (Model 11,311, Fire Testing Technology Ltd., UK).

The multiple-cycle healing behavior of the coatings deposited on glass substrates was investigated at 120 °C. A controlled scratch was introduced on the coating surface using a blade, ensuring that the damage remained confined within the coating layer and did not reach the glass substrate. The scratched samples were then placed on a pre-heated hot plate and allowed to heal at 120 °C. Three consecutive scratch-healing cycles were performed, with each subsequent scratch introduced only after the complete closure of the previous one. The healing process was monitored using a Dino-Lite digital microscope at 40× magnification.

## 3. Results and discussion

The synthesis of the DOM-MVL resin involved two consecutive reactions. First, the phenolic hydroxyl group of vanillin was methacrylated using methacrylic anhydride to obtain methacrylated vanillin (MVL). Subsequently, the aldehyde functionality of MVL reacted with the primary amine groups of DOM through a Schiff-base condensation reaction, yielding the imine-containing DOM-MVL resin. The chemical structure of the resin was confirmed by $^1$H NMR spectroscopy (Fig. S1). In particular, the appearance of signals attributable to the imine moieties confirmed the successful formation of Schiff-base linkages. These dynamic covalent bonds are expected to promote bond-exchange reactions within the crosslinked network, thus providing the vitrimer-like behavior of the final material. The preparation of the DOM-MVL/DNA coatings is schematically presented in Fig. 1a. DNA was incorporated into the DOM-MVL resin at concentrations of 10 and 20% *w*/w relative to the resin weight, together with the photoinitiator, and the resulting formulations were subsequently UV-cured to obtain crosslinked coatings and free-standing networks. For comparison, coatings based on unfilled DOM-MVL resin were also prepared. The photographs of the coatings obtained after the curing are reported in Fig. 1b-d.

Owing to its polar nature and double-helical structure, DNA showed limited compatibility with the hydrophobic DOM-MVL resin. Rather than being molecularly dispersed in the matrix, it was present primarily as discrete aggregates distributed throughout the network, as confirmed by SEM microscopy. Undoubtedly, this heterogeneous morphology represents a limitation of the present formulations. However, the approach was pursued to assess whether DNA could preserve its intrinsic char-forming activity within a bio-based, UV-curable imine vitrimer.

### 3.1. Morphological analysis of coatings

The presence of DNA aggregates within the coatings was investigated by SEM coupled with EDS. Representative cross-sectional SEM micrographs are reported in Fig. 2. While unfilled DOM-MVL coating exhibited a homogeneous and featureless morphology, the DNA-containing systems displayed the presence of dispersed domains with dimensions ranging from several tens to a few hundreds of micrometers, confirming the limited compatibility between the DNA particles and the polymer matrix. Higher-magnification images revealed that these domains were embedded within a continuous resin phase, indicating that the UV-curing process successfully produced a coherent network despite the heterogeneous distribution of the bio-based additive. The absence of analogous features in the pristine DOM-MVL sample further confirmed that these structures originated from the incorporated DNA. The nature of the aggregates was verified by EDS analysis (Fig. S2). In particular, spectra collected from the dispersed domains exhibited characteristic phosphorus signals, which are associated with the phosphate groups present in the DNA backbone. Conversely, phosphorus was not detected in either the surrounding polymer matrix or unfilled DOM-MVL coating.

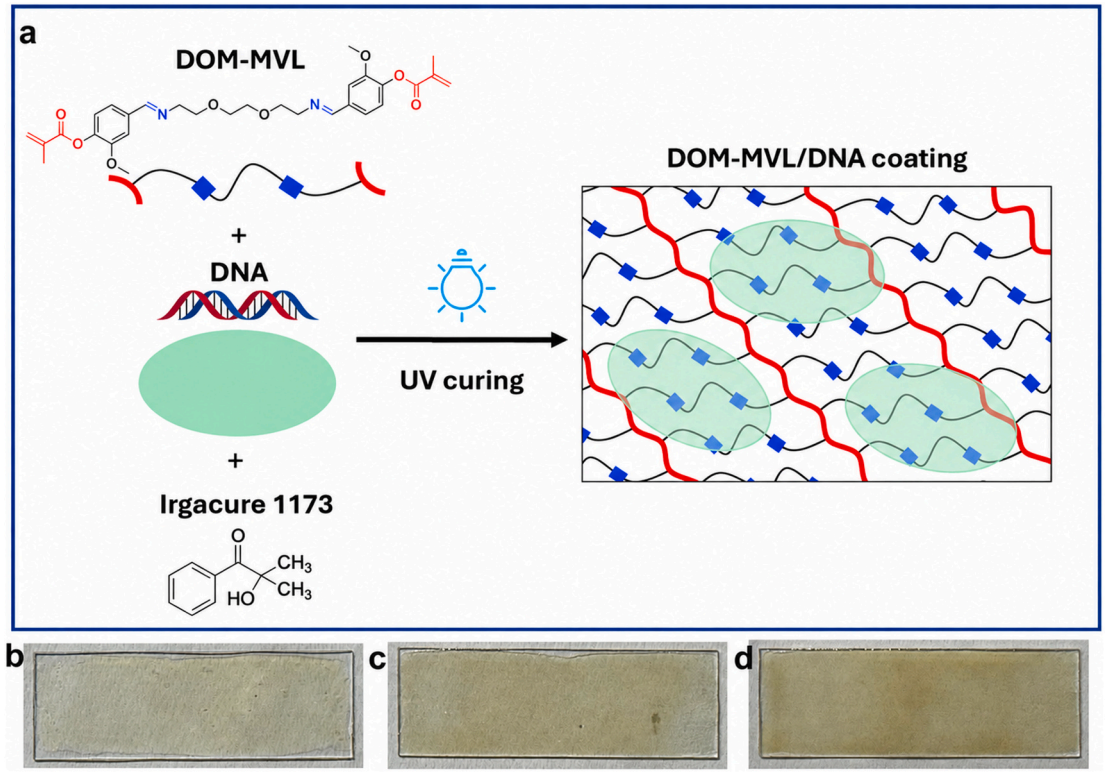



**Fig. 1.** a) Scheme of chemical structure of composite network obtained by UV curing DOM-MVL resin in presence of DNA. b-d) Photographs of the coatings deposited on glass substrates: b) DOM-MVL, c) DOM-MVL + 10% w/w, d) DOM-MVL + 20% w/w.

### *3.2. Chemical and thermal characterization of free-standing films*

The chemical and thermal characterization was performed on free-standing films obtained by mechanically peeling the cured coatings off from the aluminum substrate, as described in the Experimental Section. The chemical composition of the networks was investigated by ATR-FTIR spectroscopy (Fig. 3a). The spectra confirmed the presence of DNA within the DOM-MVL/DNA networks. In particular, the absorption band centered at 1640 $cm^{-1}$, attributed to the C═N stretching vibration of the imine functionalities present in the DOM-MVL resin [25], progressively broadened with increasing DNA content. This effect can be attributed to the overlap with characteristic vibrational bands of DNA located in the same spectral region [26–28], thus confirming the successful incorporation of the biopolymer within the vitrimeric matrix. The DSC thermograms (Fig. 3b) revealed that all formulations were rigid at room temperature, exhibiting $T_g$ in the range of 66–75 °C (Table 1). Moreover, a gradual increase in $T_g$ was observed with increasing DNA content, indicating that DNA acts as a rigid dispersed phase capable of restricting the segmental mobility of the polymer chains. The $T_g$ also suggests that the presence of DNA does not interfere with the UV-curing process, since incomplete curing would generally result in a reduction of $T_g$ due to the lower crosslinking density achieved [29].

The reinforcing effect of DNA was further assessed by DMTA. As presented in Fig. 3c and Table 1, the formulations containing DNA showed higher storage modulus values at room temperature than the unfilled DOM-MVL network, indicating an increase in stiffness. This behavior can be attributed to the intrinsically rigid DNA aggregates, which restrict chain mobility under small-amplitude deformation, in agreement with previous reports on DNA-containing polymer systems [12]. The tan δ curves (Fig. 3d) showed only limited variations in the glass transition region, with $T_g$ values of approximately 81–83 °C for DOM-MVL and DOM-MVL + 10% w/w DNA, and a slightly higher value of 87 °C for DOM-MVL + 20% w/w DNA. These results are consistent with the DSC data and substantiate the formation of highly crosslinked networks.

The thermo-oxidative stability of the materials was evaluated by thermogravimetric analyses carried out in air atmosphere (Fig. 3 e,f). All formulations exhibited a similar degradation profile characterized by three main degradation steps (Table 1), indicating that the incorporation of DNA did not significantly alter the degradation mechanism of the polymer network. The most remarkable difference among the samples concerned the final residue. While unfilled DOM-MVL network was almost completely degraded, leaving a negligible residue at 700 °C, the formulations containing DNA produced residual masses of approximately 6% w/w and 14% w/w for DOM-MVL + 10% w/w DNA and DOM-MVL + 20% w/w DNA, respectively. This behavior can be attributed to the well-known charring ability of DNA [8]. Upon thermal decomposition, the phosphate groups present in the DNA backbone convert into phosphoric acid that, in turn, promotes dehydration and carbonization reactions, favoring the formation of a thermally stable char. Simultaneously, the nitrogen-containing nucleobases contribute to the generation of non-flammable gaseous products, which justify the intumescent character of the biomacromolecule. Consequently, increasing DNA content results in a higher char yield and enhanced thermo-oxidative resistance at elevated temperatures.

The effectiveness of UV curing was further assessed by gel-content measurements. After immersion in DCM (Fig. 4a), all samples exhibited gel contents above 94%, demonstrating the formation of highly crosslinked networks with good resistance to this solvent. A different behavior was observed after immersion in water (Fig. 4b). While the unfilled DOM-MVL network maintained a gel content of approximately 94%, the values decreased to 86% and 76% for DOM-MVL + 10% w/w DNA and DOM-MVL + 20% w/w DNA, respectively. This decrease is attributed to the partial extraction of DNA, which is physically dispersed rather than covalently linked to the vitrimeric network. Owing to its hydrophilic nature, a fraction of the DNA can migrate into water during prolonged immersion, as previously observed for DNA-based flame retardant treatments on cotton fabrics [9]. These results further support

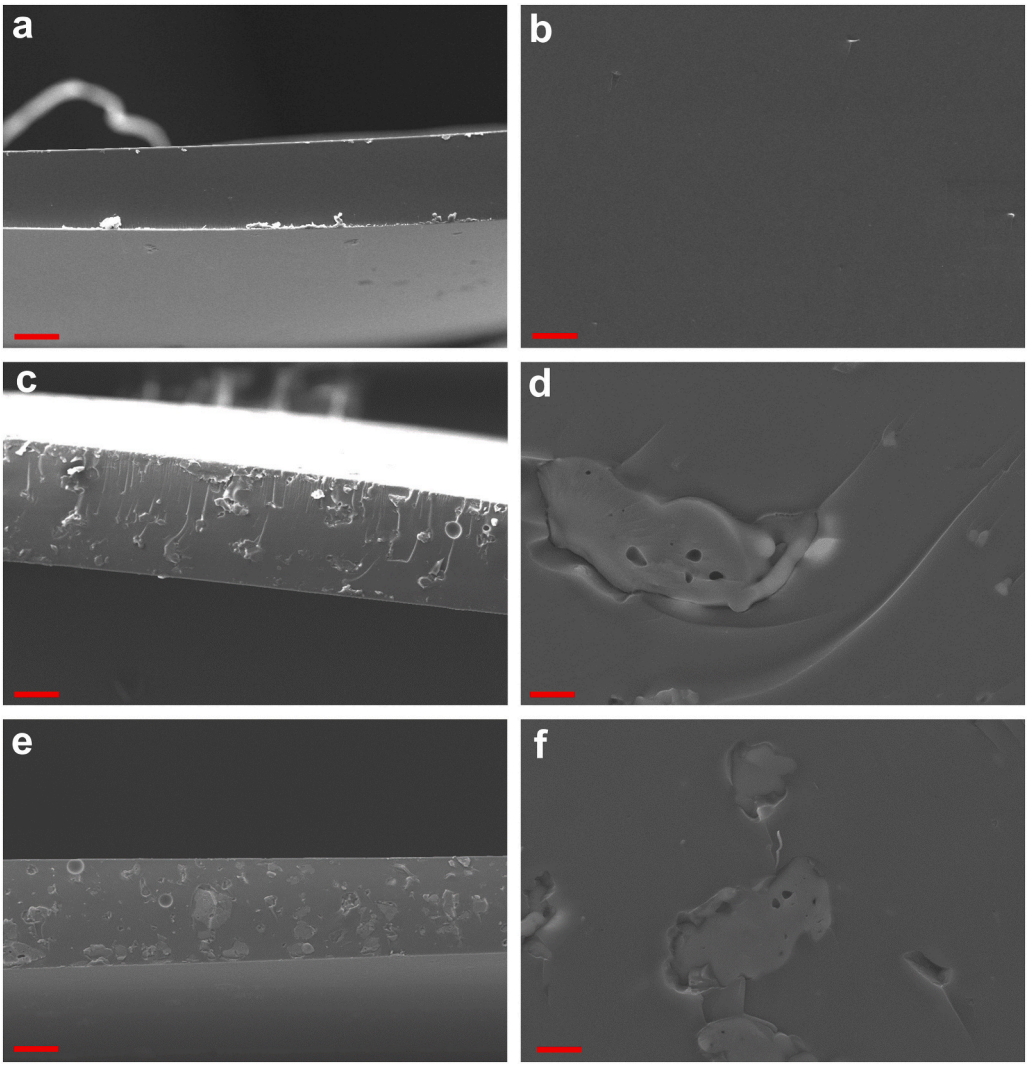



**Fig. 2.** Cross-sectional SEM micrographs of a,b) DOM-MVL; c,d) DOM-MVL + 10% w/w DNA; e,f) DOM-MVL + 20% w/w DNA. Scale bars: a, c, e) 100 μm; b, d, f) 10 μm.

the heterogeneous morphology observed by SEM and identify water durability as a limitation of the proposed coating formulations. Accordingly, the fire-performance results reported below refer to the as-prepared dry UV-cured coating formulations.

### 3.3. FR properties of the vitrimeric coatings

To assess their flame-retardant behavior, vitrimeric films were subjected to both flammability and forced-combustion tests. In the UL-94 vertical flame-spread test, all formulations, irrespective of DNA content, received an N.C. (not classified) rating because the flame rapidly propagated along the specimen and reached the upper clamp before self-extinguishing could occur. Thus, DNA incorporation did not yield a UL-94 classification under the conditions tested. Interestingly, no melt dripping phenomena were observed, indicating that the UV-cured networks retained their structural integrity during combustion.

Forced-combustion tests were carried out by cone calorimetry (CC) and pyrolysis-combustion flow calorimetry (PCFC), as documented in Fig. 5. The main thermal and smoke parameters are summarized in Tables 2–4, respectively, while the typical SEM micrographs of the residues at the end of CC tests are presented in Fig. 6.

The incorporation of DNA significantly influences the combustion behavior of the vitrimeric coatings. In particular, from CC test, both the DNA-containing formulations showed an interesting decrease in the peak heat release rate (pkHRR) with respect to unfilled DOM-MVL coating. The pkHRR decreased from 310 kW $m^{-2}$ $g^{-1}$ for the unfilled vitrimer to 239 and 192 kW $m^{-2}$ $g^{-1}$ for the formulations containing 10 and 20 wt% DNA, respectively (corresponding to reductions of 23% and 38%). A similar trend was observed for the total heat release (THR), which decreased from 7.4 to 5.1 and 4.0 kJ $m^{-2}$ $g^{-1}$ with increasing the DNA content up to 20% w/w, corresponding to reductions of 31 and 46%, respectively. These results clearly demonstrate that DNA effectively suppresses the combustion intensity of the vitrimeric matrix.

The reduction in heat release was accompanied by a decrease in time to ignition (TTI), from 19 s for unfilled DOM-MVL to 9 and 7 s for the formulations containing 10 and 20 wt% DNA, respectively. Although premature ignition is unfavorable in itself, it can be associated with the early activation of phosphorus-containing char-forming systems. In the present case, the earlier degradation onset of the DNA-containing formulations coincided with substantially higher TGA residues at 700 °C. Together with the reduced heat release, these data are likely to indicate the formation of a protective char in the condensed phase, which can limit heat and mass transfer during combustion.

The reduction in heat release was accompanied by lower smoke-related parameters. Indeed, total smoke release (TSR) progressively decreased with increasing DNA content, reaching a 73% reduction for the formulation containing 20% w/w DNA. Similarly, the specific extinction area (SEA), which is related to smoke-production efficiency,

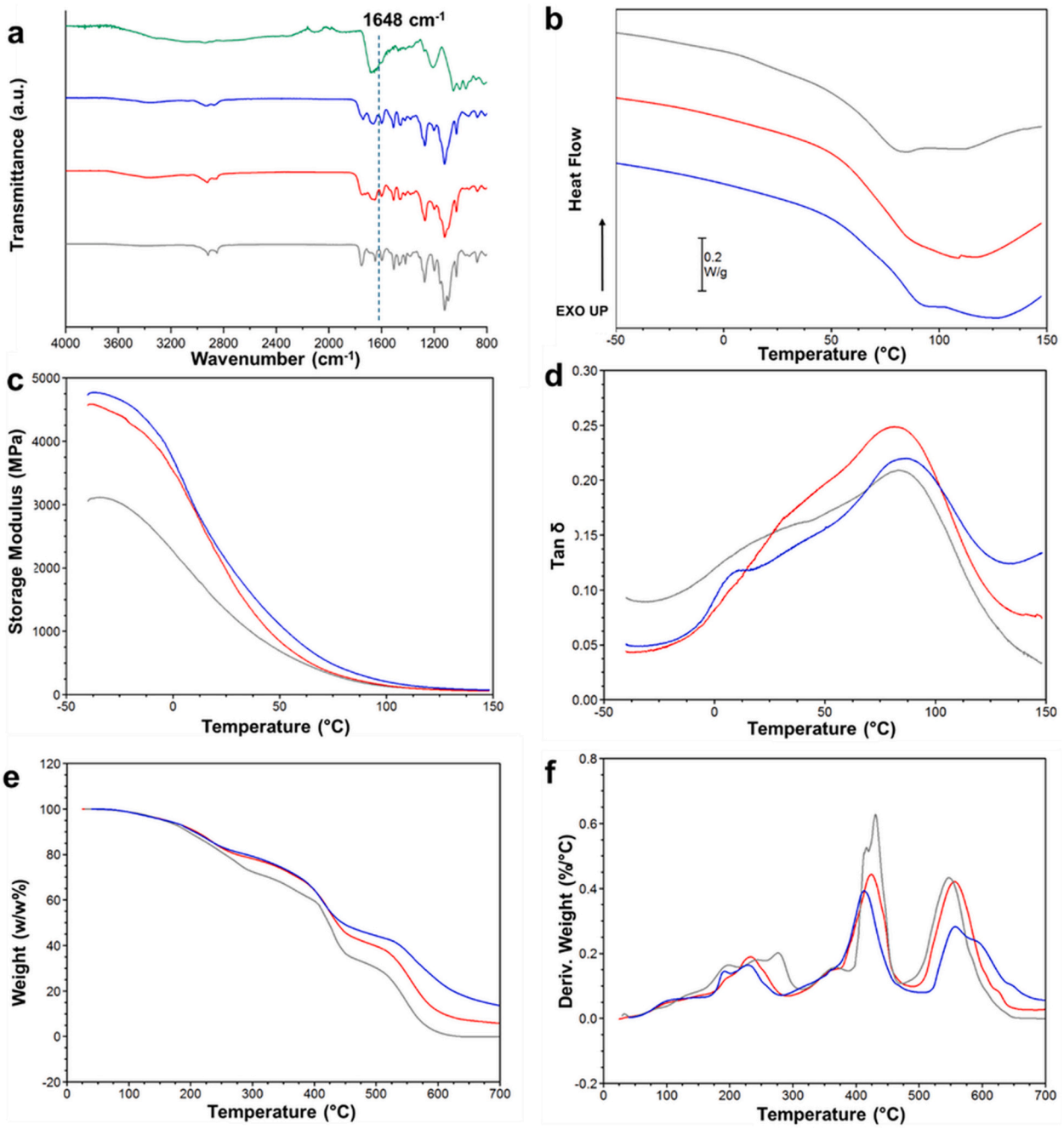



**Fig. 3.** a) ATR-FTIR spectra of DNA, DOM-MVL, DOM-MVL + 10% w/w DNA, and DOM-MVL + 20% w/w DNA networks; b) first heating DSC thermograms; c) storage modulus and d) tan δ curves obtained by DMTA; e) TGA curves in air atmosphere and f) corresponding derivative thermogravimetric curves. DOM-MVL (gray), DOM-MVL + 10% w/w DNA (red), DOM-MVL + 20% w/w DNA (blue), and DNA (green, figure a) only). (For interpretation of the references to colour in this figure legend, the reader is referred to the web version of this article.)

**Table 1**
Thermomechanical and thermal properties of DOM-MVL, DOM-MVL + 10% w/w DNA, and DOM-MVL + 20% w/w DNA networks, including $T_g$ obtained from DSC and DMTA analyses, storage modulus at room temperature, characteristic degradation temperatures, and residual mass at 700 °C.

| Sample | $T_g$ DSC (°C) | $T_g$ DMTA (°C) | Storage Modulus (MPa) | $T_{first\ deg}$ (°C) | $T_{second\ deg}$ (°C) | $T_{third\ deg}$ (°C) | Residue at 700 °C |
|---|---|---|---|---|---|---|---|
| DOM-MVL | 66 | 83 | 3.1 | 278 | 432 | 548 | 0 |
| DOM-MVL + 10% w/w DNA | 71 | 81 | 4.6 | 233 | 425 | 556 | 5.8 |
| DOM-MVL + 20% w/w DNA | 75 | 87 | 4.8 | 230 | 413 | 559 | 13.7 |

decreased from 604 to 177 $m^2\ kg^{-1}\ g^{-1}$. These findings indicate that DNA modifies the combustion process and are consistent with a greater contribution of condensed-phase charring and a reduced evolution of smoke-forming volatile products.

The PCFC results (Fig. 5c and Table 4) supported the cone calorimetry trends. DNA incorporation progressively lowered both peak heat

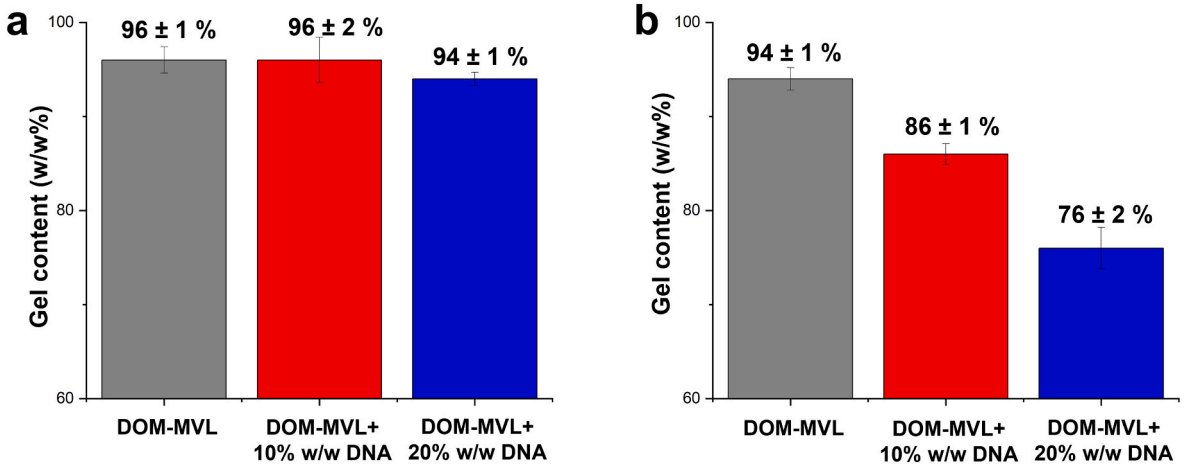



**Fig. 4.** Gel content measurements in a) DCM and b) water.

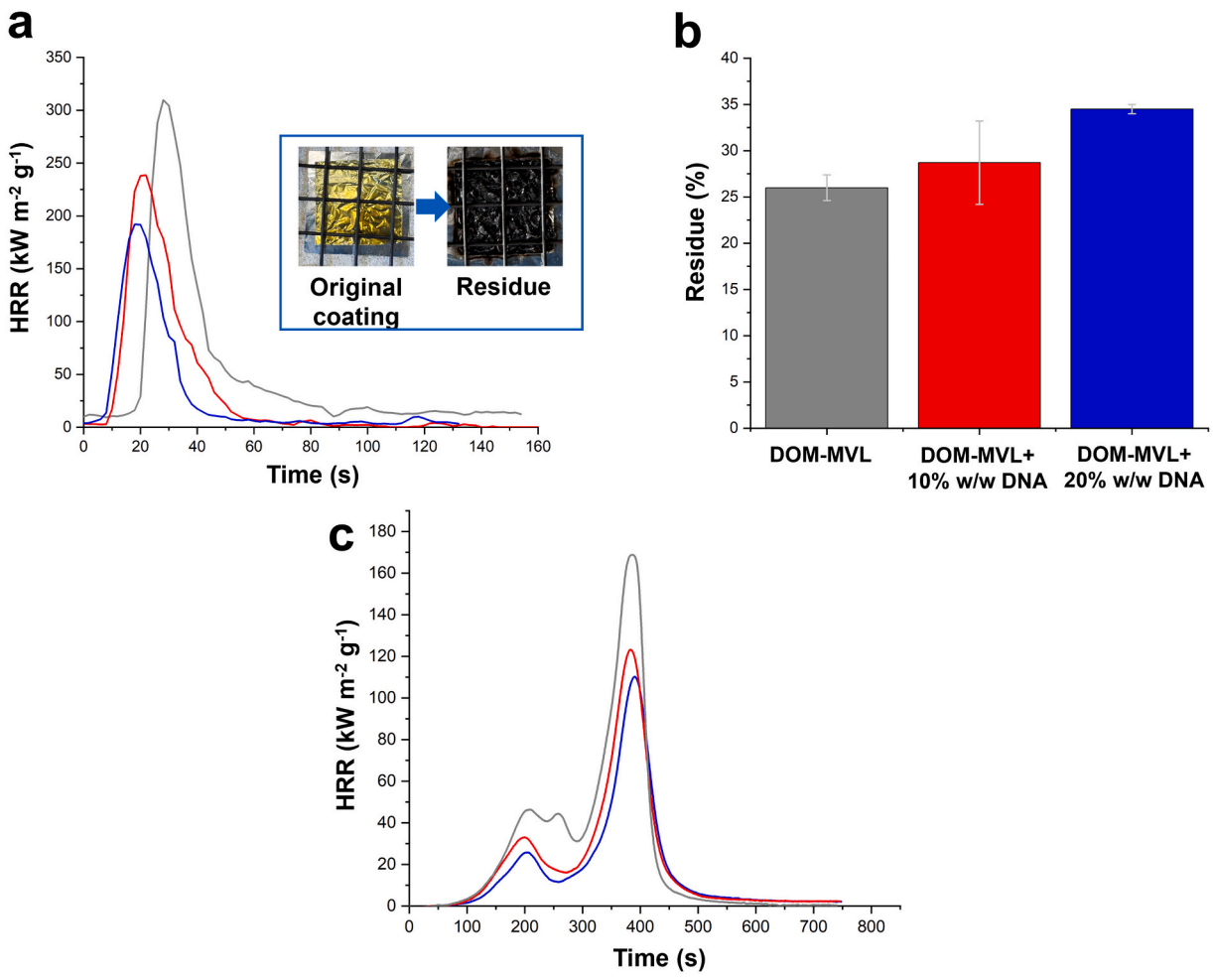



**Fig. 5.** a) HRR vs. time curves from CC tests; b) residues at the end of these tests; c) HRR vs. time curves from PCFC tests.

**Table 2**
Thermal parameters and final residues from cone calorimetry tests for the different vitrimeric coatings.

| Sample | TTI (s) | pkHRR (kW $m^{-2}$ $g^{-1}$) | ΔpkHRR (%) | THR (kJ $m^{-2}$ $g^{-1}$) | ΔTHR (%) | Residue (%) |
|---|---|---|---|---|---|---|
| DOM-MVL | 19 ± 1.4 | 310 ± 12.4 | – | 7.4 ± 1.57 | – | 26.0 ± 1.4 |
| DOM-MVL + 10% w/w DNA | 9 ± 1.4 | 239 ± 19.9 | −23 | 5.1 ± 0.83 | −31 | 28.7 ± 4.5 |
| DOM-MVL + 20% w/w DNA | 7 ± 1.4 | 192 ± 1.8 | −38 | 4 ± 1.14 | −46 | 34.5 ± 0.5 |

**Table 3**
Smoke parameters from cone calorimetry tests for the different vitrimeric coatings.

| Sample | TSR ($m^2 m^{-2} g^{-1}$) | ΔTSR (%) | SEA ($m^2 kg^{-1} g^{-1}$) | ΔSEA (%) |
|---|---|---|---|---|
| DOM-MVL | 104.5 ± 3.0 | – | 604 ± 93 | – |
| DOM-MVL + 10% w/w DNA | 96.5 ± 9.5 | −8 | 428 ± 147 | −29 |
| DOM-MVL + 20% w/w DNA | 27.9 ± 12 | −73 | 177 ± 22 | −71 |

**Table 4**
Thermal parameters and final residues from PCFC tests for the different vitrimeric coatings.

| Sample | TTI (s) | pkHRR ($kW m^{-2} g^{-1}$) | THR ($kJ m^{-2} g^{-1}$) |
|---|---|---|---|
| DOM-MVL | 81 | 169 | 9.2 |
| DOM-MVL + 10% w/w DNA | 91 | 123 | 8.3 |
| DOM-MVL + 20% w/w DNA | 99 | 110 | 7.6 |

release rate and total heat released during combustion, indicating a reduction in the inherent combustibility of the vitrimeric network. The pHRR decreased from 169 W $g^{-1}$ for unfilled DOM-MVL to 123 and 110 W $g^{-1}$ for the formulations containing 10 and 20 wt% DNA, respectively. The THR decreased from 9.2 to 7.6 kJ $g^{-1}$ at 20 wt% DNA loading. The first heat release peak, most likely associated with early decomposition of the vitrimeric network, also decreased and shifted to longer times. In combination with the TGA and residue observations, these results are consistent with the occurrence of early reactions in condensed phase promoted by DNA and a subsequent reduction of combustible volatiles [8,30].

The effectiveness of DNA as a char-promoting additive in the condensed phase was further confirmed by the residues remaining after the cone calorimetry tests (Fig. 5 b and Table 3). The residual mass increased from 26.0% for the unfilled DOM-MVL coating to 34.5% for the formulation containing 20% w/w DNA.

SEM observations of the combustion residues after cone calorimetry (Fig. 6a-f) showed significant morphological differences between unfilled DOM-MVL and the DNA-containing formulations. The residue of DOM-MVL appeared relatively discontinuous and porous, whereas the DNA-containing systems developed a more compact and coherent char. EDS analyses of the residues (Fig. S3) confirmed the presence of phosphorus-rich regions within the char, indicating that phosphorus-containing species originating from DNA remain in the condensed phase during the exposure to the irradiative heat flux. Again, together

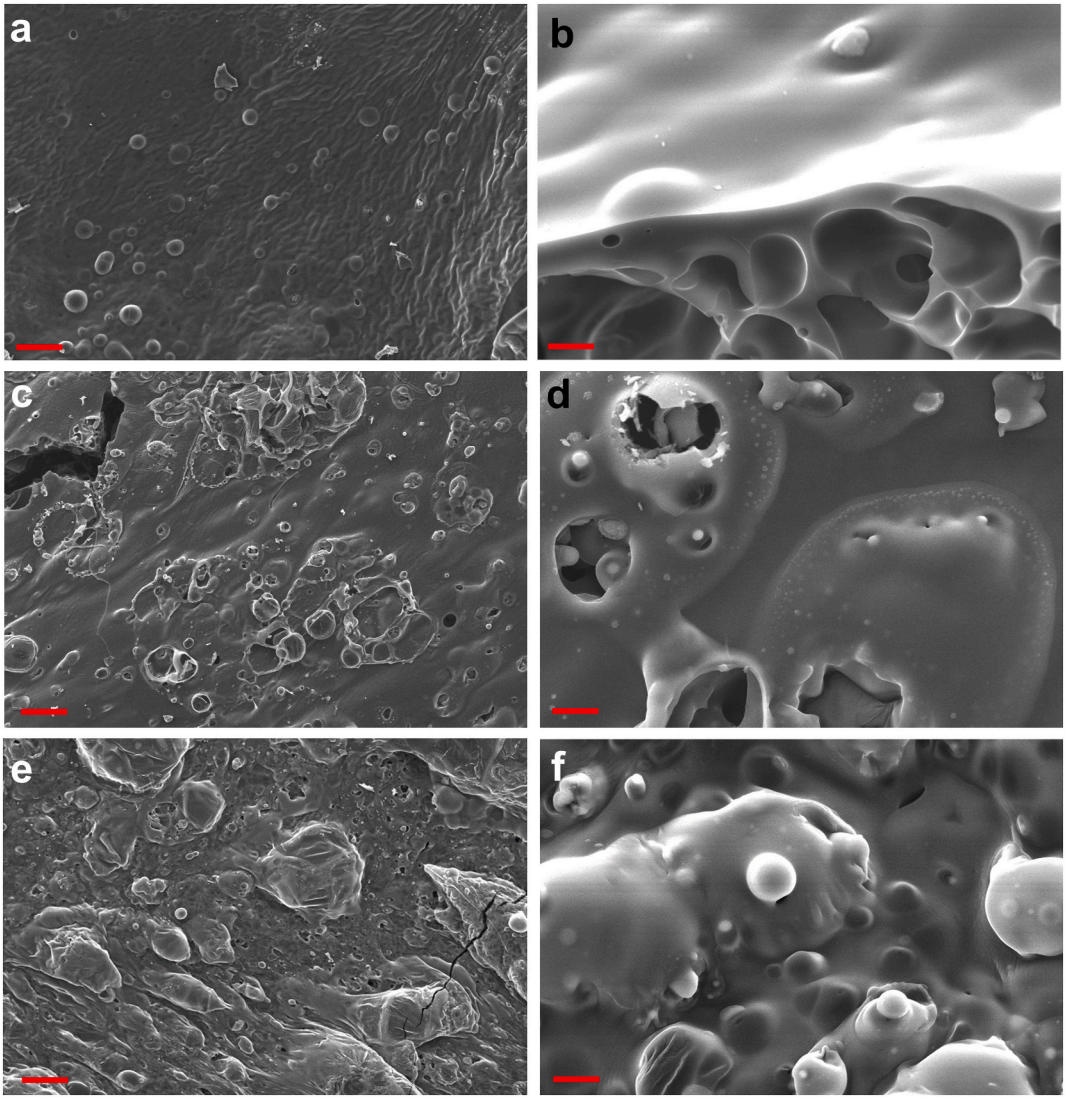



**Fig. 6.** Typical SEM images of the residues from CC tests: DOM-MVL (a,b), DOM-MVL + 10% w/w DNA (c,d), and DOM-MVL + 20% w/w DNA (e,f). Scale bars: a,c,e) 100 μm; b,d,f) 10 μm.

with the thermal and calorimetric data, these findings support the char-forming activity of DNA in condensed phase.

### 3.4. Healing properties of coatings

The multiple cycle scratch-closure behavior of coatings deposited on glass substrates was investigated at 120 °C, following the procedure described in the Experimental Section. Previous work has demonstrated the dynamic behavior of DOM-MVL-based vitrimeric networks containing reactive diluents [18]. Here, repeatable scratch closure was also observed for coatings prepared from neat DOM-MVL resin. Since 120 °C is above the $T_g$ of the formulations, this behavior may arise from the combined effects of thermally activated segmental mobility and dynamic imine exchange (whose contribution cannot be quantified independently).

As shown in Fig. 7a and Videos S1-S3, the pristine DOM-MVL coating exhibited complete scratch closure upon heating at 120 °C. The first and second scratches were completely repaired within approximately 60–70 s, while a longer healing time of about 150 s was required during the third healing cycle. The progressive increase in healing time may be attributed to the accumulation of localized network rearrangements and residual stresses induced by repeated damage-healing cycles, which can slightly reduce chain mobility in the damaged region and consequently slow down the healing process [18].

The incorporation of DNA did not prevent thermally activated scratch closure despite the heterogeneous morphology observed by SEM. For DOM-MVL + 10% w/w DNA (Fig. 7b and Videos S4-S6), the scratch closure kinetics were essentially identical to those of the unfilled network. This result indicates that the dispersed DNA aggregates do not prevent the polymer-rich continuous phase from healing the damaged region under the applied thermal treatment.

A slight increase (by about 20 to 30 s) in healing time was observed for DOM-MVL + 20% w/w DNA (Fig. 7c and Videos S7-S9). This trend is consistent with the higher glass transition temperature and storage modulus of this formulation, which imply a reduced segmental mobility, and with the larger number of DNA-rich domains that may locally slow down the polymer flow. However, complete scratch closure was observed within a few tens of seconds under the selected thermal treatment. The transimination-based chemical recycling demonstrated below and previous studies of analogous vanillin-derived imine vitrimers support the vitrimeric (dynamic) character of the network, though the proposed scratch closure experiment alone does not establish imine exchange as the exclusive mechanism.

### 3.5. Decomposition of the coatings and characterization of chemically recycled networks

As reported in literature [17,18,30], dynamic transimination reactions of imine-based vitrimeric networks can be exploited for chemical recycling purposes. Here, DOM-MVL and DOM-MVL + 20% w/w DNA coatings were subjected to chemical decomposition in excess DOM according to the procedure described in the Experimental Section. The degradation process is driven by transimination reactions, whereby the primary amine groups of DOM react with the imine bonds present in the network, progressively cleaving the crosslinked structure and generating soluble oligomeric species. The recovered oligomeric fragments were isolated and characterized by ATR-FTIR spectroscopy (Fig. S4), confirming the preservation of the characteristic chemical functionalities of the vitrimer precursor.

To demonstrate material recyclability, the recovered oligomers were subsequently mixed with a small amount of MVL and consolidated by hot pressing to obtain chemically recycled free-standing films. In the case of the DNA-containing formulation, DNA was reintroduced into the recycled material at the same concentration used in the original network

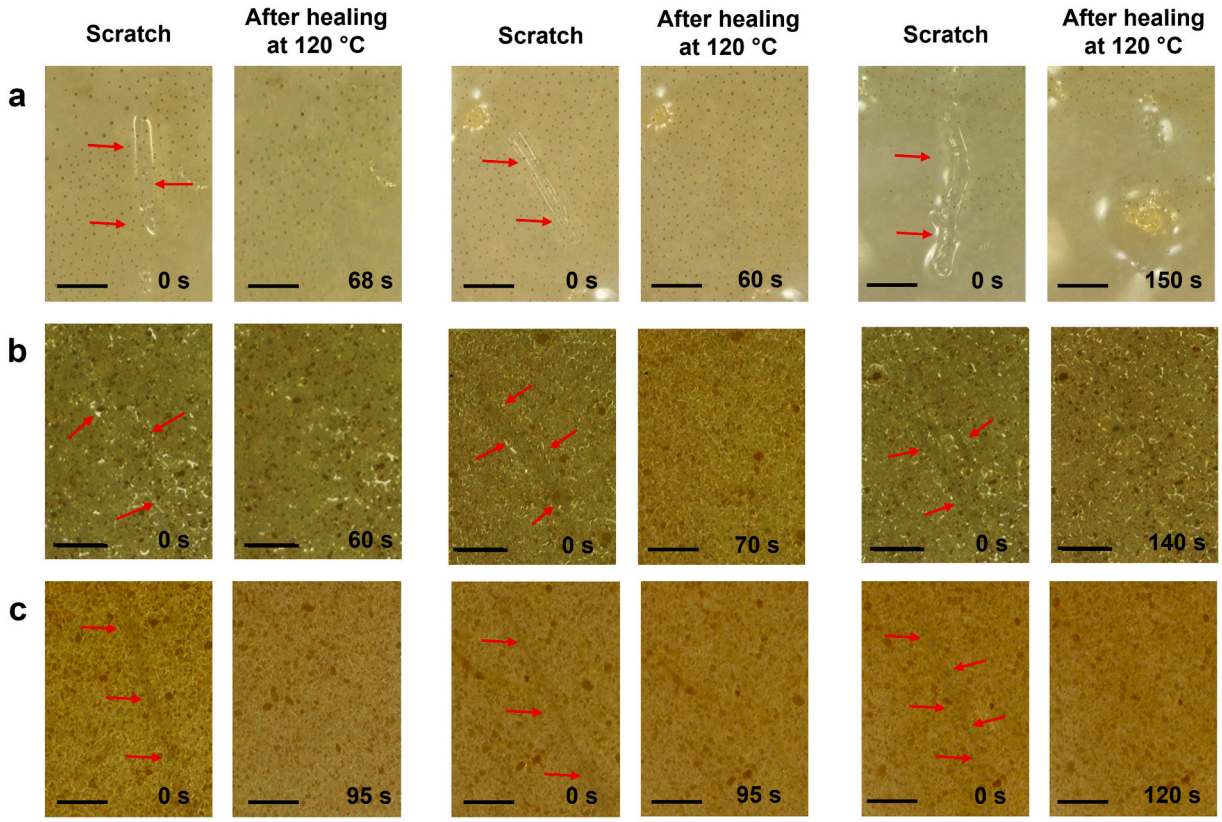



**Fig. 7.** Snapshots of scratches before and after the healing treatment at 120 °C on coatings applied on glass. a) DOM-MVL; b) DOM-MVL + 10% w/w DNA, c) DOM-MVL + 20% w/w DNA. Scale bar: 1 mm. The corresponding time points at which each snapshot was acquired are indicated in the figure.

(i.e., 20% w/w) before the hot-pressing step. Representative photographs of the recovered powder before processing and of the corresponding recycled films after hot pressing are shown in Fig. 8a. The ATR-FTIR spectra of the recycled films (Fig. S4) confirmed the successful formation of coherent materials while preserving the characteristic chemical features of the original systems.

Finally, the results from PCFC tests performed on the reprocessed samples (i.e., DOM-MVL and DOM-MVL + 20%w/w DNA) revealed a pronounced decrease in the heat release rate in presence of incorporated DNA (Fig. 8b and Table 5). Moreover, the pHRR decreased in presence of DNA, once again indicating an improvement in the intrinsic FR behavior of the coatings [8,31].

Interestingly, the reprocessed vitrimeric networks showed slightly lower pHRR and THR values than the corresponding pristine counterparts (*compare* Tables 4 and 5). Though the differences are quite small, this finding suggests that reprocessing does not affect the intrinsic flame retardancy of the vitrimeric network. The lower pHRR and THR values may be ascribed to slight changes in the network architecture promoted by transimination and hot pressing, leading to a lower generation of combustible volatile products during pyrolysis.

The TGA curves in air (Fig. 8c and d) support the interpretation of the PCFC results. More specifically, the unfilled DOM-MVL exhibited a first degradation step at lower temperature, which is consistent with the early heat-release peak observed in PCFC tests. This finding can be ascribed to the decomposition/oxidation of less thermally stable acrylic fractions, or loosely crosslinked domains within the cured network.

Upon the incorporation of 20% w/w of DNA, this first degradation event became less pronounced and the overall mass-loss profile changed significantly. This suggests that DNA modifies the degradation pathway of the vitrimeric network, promoting condensed-phase reactions rather than the release of flammable volatiles.

**Table 5**
Results from PCFC tests on the chemically recycled samples.

| Sample | TTI (s) | pHRR (W $g^{-1}$) | THR (kJ $g^{-1}$) |
|---|---|---|---|
| DOM-MVL | 73 | 120 | 7.8 |
| DOM-MVL + 20% w/w DNA | 97 | 67 | 5.0 |

## 4. Conclusions

A fully bio-based UV-curable vitrimeric formulation incorporating DNA as a sustainable flame retardant additive was designed, developed, and characterized. The combination of a vanillin-derived dynamic Schiff-base network with DNA enabled the joint assessment of flame retardancy, thermally activated scratch closure, and chemical recycling within a single material platform.

DNA showed limited compatibility with the hydrophobic resin and formed dispersed aggregates throughout the network. However, the UV-curing reaction produced coherent, highly crosslinked formulations with high gel content in DCM. DNA incorporation slightly increased $T_g$ and storage modulus of the obtained vitrimeric networks, hence indicating increased stiffness. The DNA-containing formulations showed increased char residues and lower heat release during forced-combustion tests. In particular, the formulation containing 20% w/w

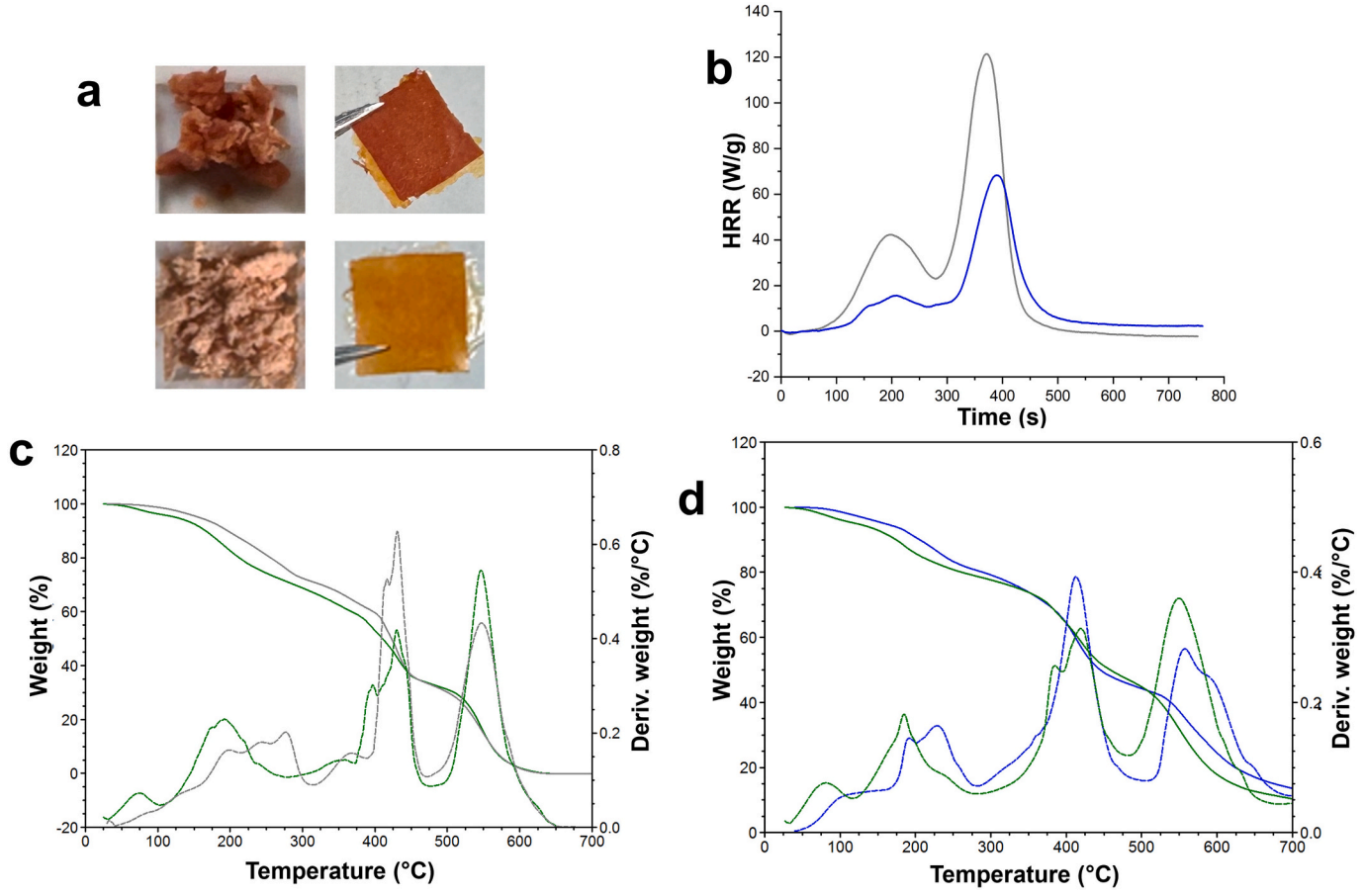



**Fig. 8.** a) Photographs of the recovered oligomeric fragments from DOM-MVL (upper raw) and DOM-MVL +20% w/w DNA (lower raw); b) PCFC tests on recycled DOM-MVL (gray), recycled DOM-MVL + 20% w/w DNA (blue); c) TGA curves (solid lines) and their first derivatives (dotted lines) in air of DOM-MVL (gray) and recycled DOM-MVL; d) TGA curves (solid lines) and their first derivatives (dotted lines) in air of DOM-MVL + 20% w/w DNA (blue) and recycled DOM-MVL + 20% w/w DNA (green). (For interpretation of the references to colour in this figure legend, the reader is referred to the web version of this article.)

DNA achieved reductions of 38% in peak heat release rate, 46% in total heat release, and 73% in total smoke release compared to unfilled DOM-MVL. SEM-EDS analyses revealed the formation of compact phosphorus-rich residues, which, together with TGA, cone calorimetry, and PCFC results, are consistent with a predominantly char-forming action of DNA in condensed phase. Nevertheless, all formulations could not be classified in UL-94 vertical flame-spread tests, despite the absence of melt dripping phenomena. DNA did not prevent repeatable thermally activated scratch closure or chemical recycling through transimination, hence highlighting a high potential of the coatings also in a view of the current circular economy approach. Building on these promising proof-of-concept results, future work will explore lower DNA loadings and optimized dispersion strategies, while assessing how sourcing from fish-processing by-products and efficient purification can support the economic feasibility and scalability of this approach.

## CRediT authorship contribution statement

**Luigi Gamberini:** Visualization, Investigation, Formal analysis, Data curation. **Anna Liguori:** Writing – review & editing, Writing – original draft, Validation, Supervision, Methodology, Investigation, Formal analysis, Data curation, Conceptualization. **Daniele Battegazzore:** Investigation, Formal analysis, Data curation. **Giulio Malucelli:** Writing – review & editing, Writing – original draft, Validation, Supervision, Methodology, Investigation, Formal analysis, Data curation, Conceptualization. **Maria Letizia Focarete:** Writing – review & editing, Validation, Supervision, Methodology, Conceptualization.

## Statement of originality

We confirm that this manuscript has not been published elsewhere and is not under consideration by another journal.

## Declaration of competing interest

The authors declare that they have no known competing financial interests or personal relationships that could have appeared to influence the work reported in this paper.

## Acknowledgments

The BIOMAPS project, HORIZON-CL4-2024-TWIN-TRANSITION-01-01 (Grant Agreement 101177344), is gratefully acknowledged. This project is funded by the European Union. Views and opinions expressed are, however, those of the authors only and do not necessarily reflect those of the European Union or HaDEA. Neither the European Union nor the granting authority can be held responsible for them.

## Appendix A. Supplementary data

Supplementary data to this article can be found online at https://doi.org/10.1016/j.porgcoat.2026.110687.

## Data availability

The raw experimental data supporting the findings of this study are available in the [AMS Acta] repository. The dataset is available at https://amsacta.unibo.it/id/eprint/9078/.

Gamberini, Luigi; Liguori, Anna; Battegazzore, Daniele; Malucelli, Giulio; Focarete, Maria Letizia (2026) Data set on Bio-based UV-curable vitrimeric coatings incorporating DNA for enhanced flame retardancy and circularity. University of Bologna. DOI https://doi.org/10.6092/unibo/amsacta/9078.

## References

[1] I.P. Okokpujie, L.K. Tartibu, H.O. Musa-Basheer, A.O.M. Adeoye, Effect of coatings on mechanical, corrosion and tribological properties of industrial materials: a comprehensive review, J. Bio- and Tribo-Corros. 10 (2024) 2, https://doi.org/10.1007/s40735-023-00805-1.
[2] A. Kausar, Polymer coating technology for high performance applications: fundamentals and advances, J. Macromol. Sci. A 55 (2018) 440–448, https://doi.org/10.1080/10601325.2018.1453266.
[3] L. Yan, Z. Xu, X. Wang, Influence of nano-silica on the flame retardancy and smoke suppression properties of transparent intumescent fire-retardant coatings, Prog. Org. Coat. 112 (2017) 319–329, https://doi.org/10.1016/j.porgcoat.2017.07.017.
[4] G. Malucelli, Surface-engineered fire protective coatings for fabrics through sol-gel and layer-by-layer methods: an overview, Coatings 6 (2016) 33, https://doi.org/10.3390/coatings6030033.
[5] Z. Yin, Z. Jiang, T. Wu, The development and application of contemporary phosphorus flame retardants: a review, Front. Mater. 12 (2025) 1508000, https://doi.org/10.3389/fmats.2025.1508000.
[6] S.V. Levchik, E.D. Weil, 3 - developments in phosphorus flame retardants, in: Woodhead Publishing Series in Textiles, Advances in Fire Retardant Materials, Woodhead Publishing, 2008, pp. 41–66, https://doi.org/10.1533/9781845694701.1.41.
[7] B.W. Liu, H.B. Zhao, Y.Z. Wang, Advanced flame-retardant methods for polymeric materials, Adv. Mater. 34 (2022) 2107905, https://doi.org/10.1002/adma.202107905.
[8] T.C. Mokhena, M.J. Mochane, E.R. Sadiku, S.S. Ray, Biomaterials as Green Flame Retardants, Springer Nature, 2024.
[9] J. Alongi, R.A. Carletto, A. Di Blasio, F. Carosio, F. Bosco, G. Malucelli, DNA: a novel, green, natural flame retardant and suppressant for cotton, J. Mater. Chem. A 1 (2013) 4779–4785, https://doi.org/10.1039/C3TA00107E.
[10] J. Alongi, R.A. Carletto, A. Di Blasio, F. Cuttica, F. Carosio, F. Bosco, G. Malucelli, Intrinsic intumescent-like flame retardant properties of DNA-treated cotton fabrics, Carbohydr. Polym. 96 (2013) 296–304, https://doi.org/10.1016/j.carbpol.2013.03.066.
[11] J. Alongi, F. Cuttica, F. Carosio, DNA coatings from byproducts: a panacea for the flame retardancy of EVA, PP, ABS, PET, and PA6? ACS Sustain. Chem. Eng. 4 (2016) 3544–3551, https://doi.org/10.1021/acssuschemeng.6b00625.
[12] O. Zabihi, M. Ahmadi, H. Khayyam, M. Naebe, Fish DNA-modified clays: towards highly flame retardant polymer nanocomposite with improved interfacial and mechanical performance, Sci. Rep. 6 (2016) 38194, https://doi.org/10.1038/srep38194.
[13] W. Denissen, J.M. Winne, F.E. Du Prez, Vitrimers: permanent organic networks with glass-like fluidity, Chem. Sci. 7 (2016) 30–38, https://doi.org/10.1039/c5sc02223a.
[14] N.J. Van Zee, R. Nicolaÿ, Vitrimers: permanently crosslinked polymers with dynamic network topology, Prog. Polym. Sci. 104 (2020) 101233, https://doi.org/10.1016/j.progpolymsci.2020.101233.
[15] M. Guerre, C. Taplan, J.M. Winne, F.E. Du Prez, Vitrimers: directing chemical reactivity to control material properties, Chem. Sci. 11 (2020) 4855–4870, https://doi.org/10.1039/d0sc01069c.
[16] A. Liguori, S. Subramaniyan, J.G. Yao, M. Hakkarainen, Photocurable extended vanillin-based resin for mechanically and chemically recyclable, self-healable and digital light processing 3D printable thermosets, Eur. Polym. J. 178 (2022) 111489, https://doi.org/10.1016/j.eurpolymj.2022.111489.
[17] L. Gamberini, A. Del Giudice, L. Papadopoulos, M.C. Righetti, M. Hakkarainen, L. Galantini, A. Liguori, M.L. Focarete, Phase organization and circularity in PLLA/vitrimer semi-interpenetrating polymer networks, Macromolecules 59 (2026) 7862–7878, https://doi.org/10.1021/acs.macromol.6c00678.
[18] A. Liguori, L. Gamberini, L. Iannucci, C. Gotti, M. Bartoli, F. Rizzi, A. Zucchelli, M. L. Curri, S. Grassini, G. Malucelli, M.L. Focarete, Multifunctional and sustainable vitrimer systems for self-healing, scratch resistance, and corrosion protection, J. Ind. Eng. Chem. (2026), https://doi.org/10.1016/j.jiec.2026.04.045.
[19] D. Wang, H. Zhang, X. Xu, Y. Qiu, G. Chang, K. Yuan, R. Xu, L. Meng, Cyclotriphosphazene based epoxy vitrimer with excellent recyclability and flame retardancy, Polym. Degrad. Stab. 238 (2025) 111346, https://doi.org/10.1016/j.polymdegradstab.2025.111346.
[20] D. Wang, R. Niu, H. Wen, Z. Zhang, Y. Liu, L. Meng, et al., Interface-engineered polyphosphazene microspheres for simultaneous enhancement of toughness and flame retardancy in bismaleimide resins, Polymer 340 (2025) 129282, https://doi.org/10.1016/j.polymer.2025.129282.
[21] A. Liguori, N.K. Kalita, G. Adamus, M. Kowalczuk, M.L. Focarete, M. Hakkarainen, Bio-based ester- and ester-imine resins for digital light processing 3D printing: the role of the chemical structure on reprocessability and susceptibility to biodegradation under simulated industrial composting conditions, Eur. Polym. J. 219 (2024) 113384, https://doi.org/10.1016/j.eurpolymj.2024.113384.
[22] Y. Xu, K. Odelius, M. Hakkarainen, Photocurable, thermally Reprocessable, and chemically recyclable vanillin-based imine thermosets, ACS Sustain. Chem. Eng. 8 (2020) 17272–17279, https://doi.org/10.1021/acssuschemeng.0c06248.
[23] A. Liguori, H. Xu, D. Hazarika, M. Hakkarainen, Simple non-equilibrium atmospheric plasma post-treatment strategy for surface coating of digital light processed 3D-printed vanillin-based Schiff-Base thermosets, ACS Appl. Polym. Mater. 5 (2023) 8506–8517, https://doi.org/10.1021/acsapm.3c01632.
[24] S. Subramaniyan, N. Najjarzadeh, S.R. Vanga, A. Liguori, P.O. Syrén, M. Hakkarainen, Designed for circularity: chemically recyclable and enzymatically degradable biorenewable Schiff Base polyester-imines, ACS Sustain. Chem. Eng. 11 (2023) 3451–3465, https://doi.org/10.1021/acssuschemeng.2c06935.

[25] A. Liguori, K.I. Garfias González, M. Hakkarainen, Unexpected self-assembly of carbon dots during digital light processing 3D printing of vanillin Schiff-base resin, Polymer 283 (2023) 126252, https://doi.org/10.1016/j.polymer.2023.126252.
[26] N.M.P. de Souza, D.K.A. da Rosa, C. de Moraes, M. Caeran, M.B. Hoffmann, E. Pozzobon Aita, L. Prochnow, A.L.A. da Motta, V.A. Corbellini, A. Rieger, Structural characterization of DNA amplicons by ATR-FTIR spectroscopy as a guide for screening metainflammatory disorders in blood plasma, Spectrochim. Acta A Mol. Biomol. Spectrosc. 310 (2024) 123897, https://doi.org/10.1016/j.saa.2024.123897.
[27] K. Szymborska-Małek, M. Komorowska, M. Gąsior-Głogowska, Effects of near infrared radiation on DNA. DLS and ATR-FTIR study, Spectrochim. Acta A Mol. Biomol. Spectrosc. 188 (2018) 258–267, https://doi.org/10.1016/j.saa.2017.07.004.
[28] C. Hansda, S.A. Hussain, D. Bhattacharjee, P.Kr. Paul, Adsorption behavior of DNA onto a cationic surfactant monolayer at the air–water interface, Surf. Sci. 617 (2013) 124–130, https://doi.org/10.1016/j.susc.2013.07.013.
[29] K.P. Menard, Dynamic Mechanical Analysis: A Practical Introduction, Second Edition, 2nd ed., CRC Press, 2008 https://doi.org/10.1201/9781420053135.
[30] A. Liguori, E. Oliva, M. Sangermano, M. Hakkarainen, Digital light processing 3D printing of isosorbide- and vanillin-based ester and ester–imine thermosets: structure–property recyclability relationships, ACS Sustain. Chem. Eng. 11 (2023) 14601–14613, https://doi.org/10.1021/acssuschemeng.3c04362.
[31] J. Alongi, A. Di Blasio, J. Milnes, G. Malucelli, S. Bourbigot, B. Kandola, G. Camino, Thermal degradation of DNA, an all-in-one natural intumescent flame retardant, Polym. Degrad. Stab. 113 (2015) 110–118, https://doi.org/10.1016/j.polymdegradstab.2014.11.001.